Experimental study on the catalytic action of heavy metals in the sulphation process and formation of black crusts by accelerated ageing tests

Valeria Comite [A*], Andrea Bergomi [A], Matteo Formenti [A], Chiara Andrea Lombardi [A,B], Mattia Borelli [A], Daniela Morale [C], Stefania Ugolini [C], Paola Fermo [A], Cecilia Cavaterra [C], Carlo Castellano [A], Cristina Della Pina [A]

[A] Dipartimento di Chimica, Università degli Studi di Milano, via Golgi 19, 20133 Milan, Italy; andrea.bergomi@unimi.it; matteo.formenti@unimi.it; chiara.lombardi@unimi.it; mattia.borelli@unimi.it; paola.fermo@unimi.it; carlo.castellano@unimi.it; cristina.dellapina@unimi.it

[B] Dipartimento di Scienze dell'Antichità, Sapienza Università di Roma, Piazzale Aldo Moro 5, 00185 Roma, Italy

[C] Dipartimento di Matematica, Università degli Studi di Milano, via C. Saldini 50, 20133 Milano, Italy; daniela.morale@unimi.it; stefania.ugolini@unimi.it; cecilia.cavaterra@unimi.it

*** corresponding author: valeria.comite@unimi.it**

Abstract

Research conducted on the degradation of cultural and architectural heritage caused by the deposition of air pollutants indicates that the deterioration of carbonate materials is due primarily to the interaction of the substrate with sulphur dioxide (SO_2) and particulate matter (PM) deriving from the combustion of fossil fuels. The main chemical degradation process is the sulphation of the substrate, which consists in the initial conversion of SO_2 into sulphuric acid (H_2SO_4) and the subsequent reaction of this product with calcium carbonate ($CaCO_3$). This leads to the formation of black crusts composed mainly of gypsum ($CaSO_4 \cdot 2H_2O$), inside which PM is embedded. These carbonaceous particles also contain heavy metals that can act as catalysts in both stages of the sulphation process, favouring the degradation of the substrate. However, the degree to which each specific metal is able to affect sulphation is still unclear. This research aims to evaluate which heavy metals activate the sulphation process by carrying out targeted exposure mock-up tests in special climatic chambers. The selected cations were the following: Fe^{3+}, Cu^{2+}, Mn^{2+}, Pb^{2+}, Cr^{3+}, V^{5+} (deposited concentrations were calculated based on data from urban PM). In addition, mixtures involving three or more metal cations were also used to evaluate possible synergistic effects. Finally, PM2.5 extracted from quartz-fibre filters sampled in the city of Milan was also included in the experimentation. The physicochemical characterization of the different mock-up samples was performed both in the pre-exposure and post-exposure phases using different analytical techniques such as: colorimetric analysis, stereomicroscopic observations, SEM-EDX (Scanning Electron Microscopy coupled to Energy Dispersive X-Ray Spectroscopy), IC (Ion Chromatography), and XRPD (X-ray powder diffraction). Results show that some metal cations (Pb, Cu, Cr) are able to activate the catalytic process faster than others (Fe, Mn). Also, samples treated with metal mixtures and PM2.5 exhibited the greatest catalytic action, highlighting a synergistic effect of more heavy metals acting together.

Keywords: black crusts, calcium carbonate degradation, sulphation process, accelerated aging chambers, catalytic action of metals

1. INTRODUCTION

In recent decades a rapid deterioration of the artistic, cultural, and environmental heritage has been observed. The degradation of the materials is a complex phenomenon which can be ascribed to several factors, both natural and anthropogenic. In most cases this occurs gradually, but irreversibly, and begins at the very moment in which the work of art is created. Research conducted on the degradation of carbonate materials shows that they are particularly susceptible to the presence of water and to the surface deposition of sulphur dioxide (SO_2) and particulate matter (PM), which are air pollutants produced primarily by the combustion of fossil fuels and present in high concentrations in urban

polluted environments. Another significant source of atmospheric sulphur is represented by non-ferrous ore smelting processes, in which sulphur impurities are oxidized to SO_2 (Fassina et al., 1988).

Black crusts are complex layers that form on stone surfaces due to the deposition and reaction of SO_2 and PM with the carbonate substrate. These layers are typically stratified, with the outer ones being rich in gypsum, carbonaceous particles, and other species, while the inner layers usually contain unreacted calcite and other components from the undamaged stone. The composition, morphology, and stratification of black crusts are influenced by the surrounding environmental conditions and the chemical nature of the pollutants involved. Being one of the most widespread degradation phenomena concerning built cultural heritage in outdoor environments, this type of deterioration has been the object of various studies (Amoroso and Fassina 1983; Bonazza et al. 2007; Brimblecombe 1999, 2000; Del Monte et al. 1981; Turkington et al. 1997; Zappia et al. 1998).

A key mechanism in the formation of black crusts is the well-known sulphation process, which is initiated by the presence of SO_2, which is then oxidized to sulphur trioxide (SO_3), which in turn reacts with water to form sulphuric acid (H_2SO_4). In the final step, this product reacts with calcium carbonate ($CaCO_3$) in the stone to form gypsum ($CaSO_4 \cdot 2H_2O$), a primary component of black crusts. The different chemical reactions involved in the sulphation process are well-documented in literature. Beilke and Gravenhorst (1978) investigated the heterogeneous oxidation of SO_2 in the droplet phase, which was fundamental in understanding the formation of sulphuric acid under atmospheric conditions. Lancia et al. (1991) and Sada et al. (1982) further studied the processes of dissolution and absorption of calcium carbonate and calcium sulphite in the presence of SO_2, providing essential knowledge to better describe the sulphation mechanism. In particular, Verges-Belmin (1994) introduced the concept of pseudomorphism in the context of marble sulphation, where gypsum forms while preserving the original crystalline morphology of calcite. This characteristic provided critical insights into the different degradation patterns and the extent of sulphation.

Nitrogen oxides (NO_x), commonly present in polluted urban atmospheres, can also significantly influence the sulphation rate of calcareous materials. Following several atmospheric reactions, NO_x is converted into nitric acid (HNO_3), which enhances the acidity of the system and therefore accelerates the dissolution of calcium carbonate and consequent gypsum formation. NO_x can also have an indirect effect in the rate of the sulphation process by acting as catalysts in the oxidation of SO_2 to SO_3 (Bozkurt et al., 2002). The catalytic effect of NO_x is particularly evident in areas where vehicular emissions and industrial activities are the main pollutant sources. While this study does not investigate the impact of NO_x on the sulphation process, it is crucial to acknowledge its potential role in accelerating the degradation of stone materials exposed to polluted urban atmospheres. Future research should consider the combined effects of NO_x and SO_2 to evaluate a possible synergistic impact.

The sulphation process can also be promoted by other species acting as catalysts, including various heavy metals adsorbed on carbonaceous particles. Other authors, such as Delegou et al. (2018), Belfiore et al. (2013), and La Russa et al. (2016), highlighted that the morphology of the layers and the enrichment in heavy metals within the black crusts are influenced by factors such as the sampling height, the deposition surface, the different accumulation times of pollutants, the varying exposure to pollution sources, and washing. Understanding the mineralogical and chemical composition of black crusts is essential in order to develop effective stone conservation strategies.

In-depth studies on the formation mechanisms of black crusts, such as the one carried out in this study, are also important. In this regard, different approaches have been used in literature studies concerned with this issue:- the first one involves the physicochemical analysis of *real-life* black crusts sampled from historical monuments and buildings in order to determine the type of pollutants that

lead to their formation (Bugini et al, 2000; Bonazza et al., 2005; Comite at al., 2021; Gavino et al., 2004; La Russa et al., 2013; Maravelaki et al., 2004; McAllister et al., 2005, 2006, 2008; Ruffolo et al., 2015; Toniolo et al., 2009);

- another approach consists in the exposure of carbonate substrate specimens to outdoor environments for prolonged time ranges (Comite et al., 2017; Fermo et al., 2018; Zappia et al., 1998;), allowing to relate the sulphation process to the local environment and air pollution characteristics;

- lastly, black crust formation can be studied by carrying out tests in accelerated aging chambers ('climate chambers') (Ausset et al., 1996, 1999; Boke et al., 1999; Elfving et al., 1994, Hutchinson et al.,1992).

One of the main results arising from these studies was uncovering the ability of PM to act as a catalyst in the conversion of sulphur dioxide to sulphuric acid (Mc Allister 2008). However, the specific role of the various constituents of PM is still unclear. Some studies started to tackle the issue (Novakov et al., 1974; Rodriguez-Navarro and Sebastian 1996; Elfving et al., 1994) indicating metal oxides, salts, and the carbonaceous fraction of PM (organic carbon and elemental carbon) as the species responsible for catalysis, but the role of specific species is yet to be defined.

In this regard, the present research introduces our first study on how the sulphation process is affected by the catalytic action of metal cations commonly found in PM. More specifically, mock-up samples of Carrara marble treated with aqueous solutions of metal cations (namely: Fe^{3+}, Cu^{2+}, Mn^{2+}, Pb^{2+}, Cr^{3+} and V^{5+}) and elemental carbon (EC) were exposed in special climate chambers. Samples treated with urban particulate matter were also tested under the same experimental conditions for comparison. The exposure was conducted using identical cycles for each test in the presence of SO_2, relative humidity, and Xenon light. The only parameter which varied between the tests was the nature of the metal or metal mixture under examination. A physicochemical characterization of the mock-up samples was carried out both pre- and post-exposure through a multi analytical approach using Scanning Electron Microscopy coupled with Energy Dispersive X-ray spectroscopy (SEM-EDX); colorimetric analysis; Ion Chromatography (IC) and X-Ray Powder Diffraction (XRPD).

This research work is part of a larger inter-departmental project of the University of Milan, entitled SciCult, (Call SOE-SCICULT 2020 - "Mathematical modeling and SCIentific analysis for CULTURAL HERITAGE: prediction and prevention of chemical and mechanical degradation of monumental stones in outdoor environments"), whose final goal is to develop a mathematical model and statistical techniques capable of predicting the formation and growth of black crusts in relation to a given environmental context. The approach presented in this paper represents a first step in this direction by providing essential experimental data for insights into the chemical and mechanical degradation processes of monumental stones, thus enhancing the predictive capabilities of the models being developed.

2. MATERIALS AND METHODS

2.1. Marble Samples

The mock-up samples used in this study were made of white Carrara marble (provided by Alberto Giananti's "Marble Ornament" company based in Carrara, Italy). This substrate was chosen as the reference carbonate material since it is one of the most frequently used marbles in fine arts and architecture worldwide. Specifically, the samples were cut into 3x3x1cm specimen and treated to increase surface roughness, thus improving the adhesion of the target compounds. Moreover, the edges of all samples were covered with silicone gel to eliminate any trigger points (Giavarini et al., 2008) which may favour degradation and therefore affect thereproducibility of the data. The number of specimens (88) was selected based on the size of the climatic chambers and allowed to conduct a comprehensive analytical characterization.

2.2. Selection of metal cations, preparation of aqueous solutions and deposition on samples

Prior to exposure in the accelerated aging chambers, marble mock-up samples were treated with a series of metal aqueous solutions and urban particulate matter (Table 1). The choice of metal cations was made based on the species commonly found in urban PM: Fe^{3+}, Cu^{2+}, Mn^{2+}, Pb^{2+}, Cr^{3+} and V^{5+} (McAllister et. al., 2008; Grgic et al., 1992; Martins et al., 1999; Brandt and van Eldik et al., 1995). Moreover, all of these metals are known to act as catalysts towards S(IV) oxidation and their role in the sulphation process has already been hypothesized (Brandt, C., van Eldik, R., 1995; Grgic et al., 1992; Martins at al., 1999; Vidal, et al., 2019).

In addition to assessing the catalytic ability of individual metals, the synergistic action of multiple species was also taken into account by carrying out experiments with mixtures of selected cations (Table 1). Indeed, this phenomenon has already been demonstrated in some literature studies. (Brandt and van Eldik, 1995; Boke et al., 1999; Grgic et al., 1992; Hutchinson ey al., 1992; Martins at al., 1999). Specifically, the three mixtures used were: Fe^{3+}, Cu^{2+}, V^{5+} (labelled as "M1"); Fe^{3+}, Mn^{2+}, Pb^{2+}, Cr^{3+} (labelled as "M2"); and Fe^{3+}, Cu^{2+}, Mn^{2+}, Pb^{2+}, Cr^{3+}, V^{5+} (labelled as "M3"). Finally, PM 2.5 sampled in the city of Milan was also extracted and deposited as a solution on marble specimens in order to compare the action of *real-life* PM with the aqueous solutions. Particulate matter was extracted from the quartz-fibre filters using a procedure reported in Bergomi et al., 2022.

All selected metals, mixtures and PM2.5 were deposited in solution. The concentration of the different cations was calculated based on the composition data from urban particulate matter (PM 2.5 sampled on filters in the city of Milan) (Bergomi et.al., 2022). This is shown in Table 1 (expressed in ppm), together with the starting compound used as the metal source. In the case of PM2.5, 10 mg of extracted particles were deposited on the surface of each sample, in agreement with the concentrations used in other similar studies (Ausset et al., 1996, 1999; McAllister et al., 2008; Rodriguez-Navarro and Sebastian 1996). The same tests were conducted in parallel also on blank mock-up samples (labelled as "B"), which consisted of the marble substrate as such.

Table 1 – Metal aqueous solutions and urban PM2.5 used to treat the marble mock-up samples.

Solution	Concentration / ppm	Starting compound
Fe	2000	Fe_2O_3
		$Fe(NO_3)_3 \cdot 9H_2O$
Cu	100	$CuCl_2 \cdot 2H_2O$
Mn	200	$MnCl_2 \cdot 4H_2O$
Pb	70	$PbCl_2$
Cr	40	Cr_2O_3
V	30	V_2O_5
M1	Fe: 2000 Cu: 100 V: 30	Fe_2O_3 $Fe(NO_3)_3 \cdot 9H_2O$ $CuCl_2 \cdot 2H_2O$ V_2O_5
M2	Fe: 2000 Mn: 200 Pb: 70 Cr: 40	Fe_2O_3 $Fe(NO_3)_3 \cdot 9H_2O$ $MnCl_2 \cdot 4H_2O$ $PbCl_2$ Cr_2O_3
M3	Fe: 2000 Mn: 200 Pb: 70 Cr: 40 Cu: 100	Fe_2O_3 $Fe(NO_3)_3 \cdot 9H_2O$ $CuCl_2 \cdot 2H_2O$ $MnCl_2 \cdot 4H_2O$ $PbCl_2$

	V: 30	Cr_2O_3 V_2O_5
PM	1.11 mg cm^{-2}	Urban PM (Milan)

The mock-up samples were treated by depositing the solutions on the surface of the samples (Fig. A1 supplementary material), followed by the addition of graphite (5-10% wt. with respect to PM mass). This was done to simulate elemental carbon (EC) present in atmospheric particulate matter, which may favour the sulphation process acting as a support for the metals.

2.3. Accelerated aging chambers tests ('climate chambers')

Since the catalytic action can be influenced by several factors other than the type of metal directly involved in the catalysis, such as experimental conditions, metal oxidation states, relative oxidation-reduction capacity, pH, and temperature (Giavarini et al., 2008; Grgic et al., 1992), it is important to study the oxidation process under conditions that can best simulate real-life conditions. For this reason, following the sample preparation described in the previous section, marble specimens were exposed in two special climatic chambers for corrosion and light irradiation tests. The corrosion chamber provided the source of SO_2 (ambient temperature 25°C) under a strong humid atmosphere, in line with literature data (Allen et al., 2000; Ausset at al., 1999; Boke et al., 1999; Cobourn, 1993; Hutchinson et al., 1992; Spiker et al., 1992, 1995). Instead, the light irradiation chamber simulated the full spectrum of natural sunlight by xenon arc irradiation. For this purpose, the following climatic chambers were provided by Innovhub Stazioni Sperimentali per l'Industria s.r.l. (Milan, Italy): a Humidity cabinet D200 (S.N. 201) automatic damp heat chamber with SO_2 from CO.FO.ME.GRA srl and a Q-Sun Xe-3, xenon arc chamber from Q-Lab Corporation (Comite at al., 2022). The use of both aging chambers is important in these types of studies (Wittkowski et al., 2014; Price & Brimblecombe, 1994) as it allows a more realistic simulation of the outdoor environment and also leads to an increase in temperature, which can affect the catalytic mechanism of the metal cations. SO_2 corrosion tests in wet atmosphere were conducted following the ISO 22479:2019 technical standard and included SO_2 (0.67% v/v) and relative humidity (80±10%) with the following exposure cycle: 4 hours in test condition, 2 hours in ambient condition. The irradiation test was carried out following the UNI EN ISO 4892-2:2013 technical standard using a light source consisting of 3 xenon 1500W lamps at UV irradiance (0.68 ± 0.02) (W/m2nm), internal chamber temperature (38 ± 3) °C.

These operating parameters were applied to a precise exposure cycle/week: 48 hours of corrosion in a wet atmosphere with sulphur dioxide; 24 hours of exposure to xenon arc light; 72 hours of corrosion in a wet atmosphere with sulphur dioxide; 24 hours of exposure to xenon arc light. This exposure scheme was repeated for a total of four weeks and at the end of each week the mock-up samples were retrieved for analysis. Two identical sets of each sample were tested (Fig. 1) and the samples were numbered in ascending order. The PM 2.5 series is reported as an example:

- PM1 / PM 2: 1 week of exposure
- PM 3 / PM 4: 2 weeks of exposure
- PM 5 / PM 6: 3 weeks of exposure
- PM 7 / PM 8: 4 weeks of exposure

All the other samples follow the same labelling scheme (Fig. 1).

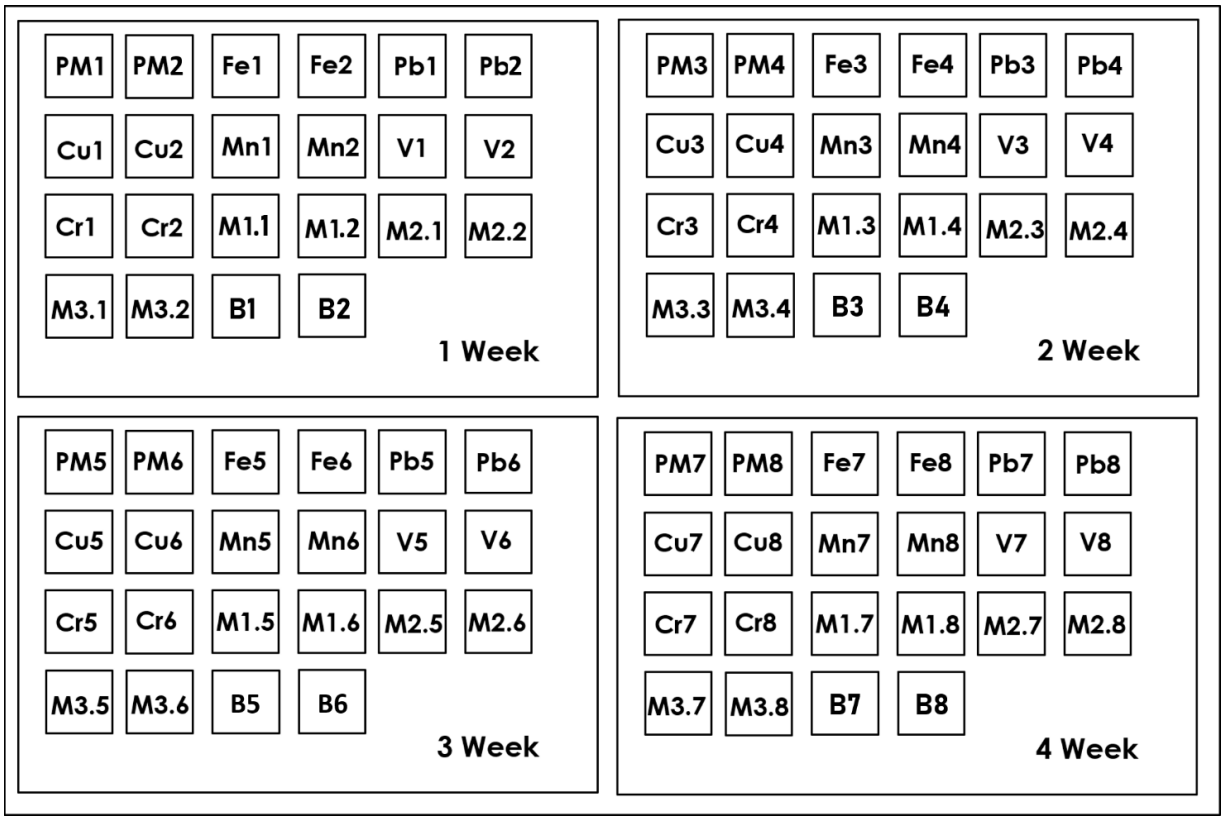

Fig.1 Sampling/labelling scheme for the 4-week exposure tests.

2.4.Analytical techniques for samples characterization

The physicochemical characterization of the different specimens was performed both in the pre-exposure and post-exposure phases using different analytical techniques such as colorimetric analysis, SEM-EDX, IC, and XRPD. Also, macroscopic observations were carried out prior to all others to verify the presence, distribution, and amount of gypsum on the surface of the specimens. Details of the techniques employed are listed below:

- Colorimetric analyses were carried out by means of a Konica Minolta CM 2600d portable spectrophotometer, referring to the CIE L* a* b* chromaticity diagram and the UNI EN 15886 (2010-Conservation of cultural property - Test methods - Colour measurement of surfaces) technical standard. L* is the luminosity, which varies from black (value = 0) to white (value = 100); a* ranges from +a*(red) to –a*(green) and b* varies from +b* (yellow) to -b* (blue).

- SEM-EDX analyses were performed with a Hitachi TM-4000 scanning electron microscope equipped with a 4-quadrant BSE (back-scattered elections) detector, a low-vacuum SE (secondary electrons) detector, and an Oxford AztecOne EDX. By utilizing low vacuum conditions, images could be obtained without metallization of the sample. Vacuum charge reduction (L) was employed to preserve samples for further analysis. Observations were made at different magnifications (30X, 100X, 250X, and 300X) and acquired in BSE mode. For each sample, EDX spectral element maps were acquired in false colors. The Oxford AZtecOne EDX system offers the standard windows integral mapping mode, where the area of each peak in the spectrum is summed to identify the elements present and their concentration. Additionally, the system features a second mapping mode called TruMap, which is suitable for specimens with overlapping peaks. This approach uses deconvolution to fit the element peak shapes across the entire spectrum for each pixel in the EDX map. It provides the benefit of resolving overlapping peaks and automatically eliminating data artefacts and false background variations. Map Acquisition Settings provided a resolution of 512 pixels to acquire maps in more detail, an acquisition time of 50 frames (passes over the map area),

and the processing time set to 'Sensitive' mode to process the x-ray signal from the EDX detector and removing noise. The pixel dwell time was set to 100 µs. Map acquisitions were performed at an acceleration voltage of 15 kV and at different magnifications (25X, 50X, 100X, 150X).

- IC was employed for the quantification of the main inorganic constituents of the deposits. About 2 mg of powder was placed in a test tube and treated with 10 mL of Milli-Q water (Fermo et al., 2015). The solutions were put in an ultrasonic bath for 1 h, then they were centrifuged for 3 min and injected for IC analysis. Measurements were carried out using an ICS-1000 HPLC system equipped with a conductivity detector.

- The crystalline phase composition of the powders was determined by XRPD by means of a Rigaku Miniflex 600 diffractometer at the CuKα wavelength performing a continuous scanning with a scattering angle 2θ range of $10°<2\theta<80°$, using a randomly oriented powder mount. Analyses were performed on the gypsum powder collected from the surface of the specimens and on the surface of the samples after the powder was removed surface investigated on the specimen is 2 cm^2).

3. RESULTS AND DISCUSSIONS

3.1.Macroscopic observation

The results obtained by macroscopic observations after the exposure cycles (Fig. 2a) show abundant formation of gypsum crystals on the surface of almost all the samples as early as the first week. The specimens that showed the greatest amount of gypsum formation were those treated with the M2 solution, M3 solution, and PM 2.5. Instead, smaller amounts of gypsum were observed for mock-up samples treated with V, Cu and M1 solutions. These initial observations suggest that the mixtures have a higher catalytic effect than the individual cations.

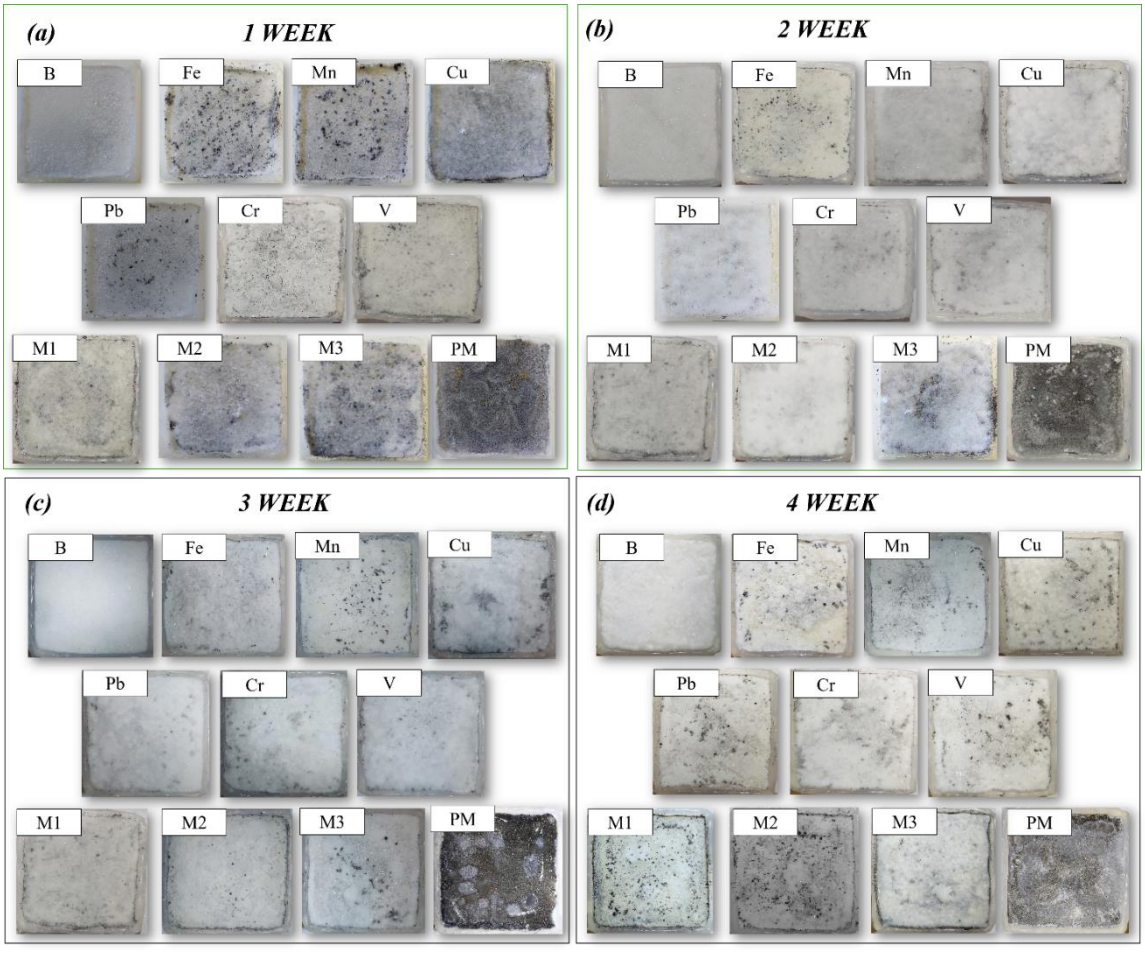

Fig. 2 Images of samples taken during the 4-week exposure in the accelerated ageing chambers

In the second week of sampling (Fig. 2b), a slight increase in acicular *habitus* crystals of gypsum was observed on the surface of all samples. . This was the case particularly for samples treated with Pb, suggesting a delayed catalytic action of this cation. An increase in gypsum crystals also appears evident for the M3 mix, in contrast to the Fe-treated sample, which developsfewer crystals.

In the third week (Fig. 2c), gypsum seems to compact, creating concretion-like structures that appear to be heterogeneously distributed over the entire surface. These larger aggregates are evident in the M3 and PM 2.5 samples (see the Fig. A2 supplementary materials). This phenomenon is observed to a greater extent after 4 weeks of exposure for all specimens (Fig. 2d). Moreover, observation of the surfaces after week 4 shows that the acicular crystals tend to stratify, creating organized structures that resemble white- gypsum crusts (see Fig. A2 Supplementary materials, stereomicroscope images).

This initial investigation shows that Pb, Cu and Cr are more active towards sulphation than the other species taken individually and that mixtures of metal cations, particularly M2 and M3, display a synergistic action that is similar to the one observed for PM2.5, in agreement with similar literature studies (Brandt and van Eldik, 1995; Grgic et al., 1992; Martins at al., 1999).

3.2.SEM-EDX analysis

SEM analyses enabled to observe the surfaces of the mock-up samples during the four-week exposure tests. These observations shows that almost all the specimens were completely covered with gypsum crystals after one week of exposure. Moreover, the number of crystals increased in the second and third weeks, whereas in the final week, in addition to the formation of new crystals, there was also an increase in thickness, shape and distribution of gypsum crystals. Furthermore, as suggested in other literature works (Ausset at al., 1999), the results show that that the nucleation of gypsum crystals (Fig. 3) is favoured in areas where graphitic carbon is present. Indeed, Cheng et al. (1987) observed that carbon particles collected from combustion sources accelerated the sulphation reaction of marble.

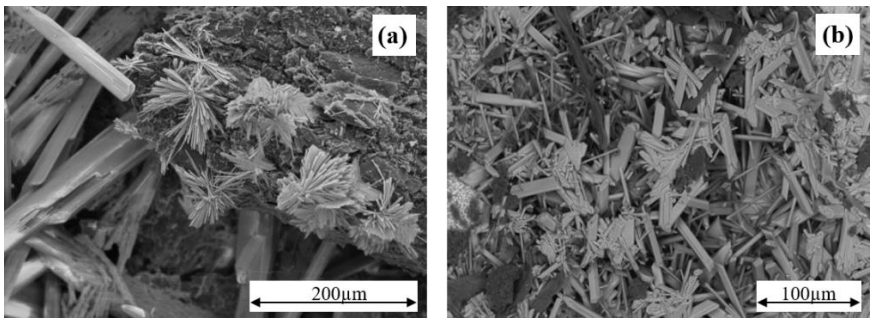

Fig.3 BSE image showing the nucleation of gypsum on carbon particles. . (a) scale bars 200 µm; (b) scale bars 100 µm.

As an example, Fig. 4 shows the observations made on representative samples observed by SEM in the first and fourth week of exposure.

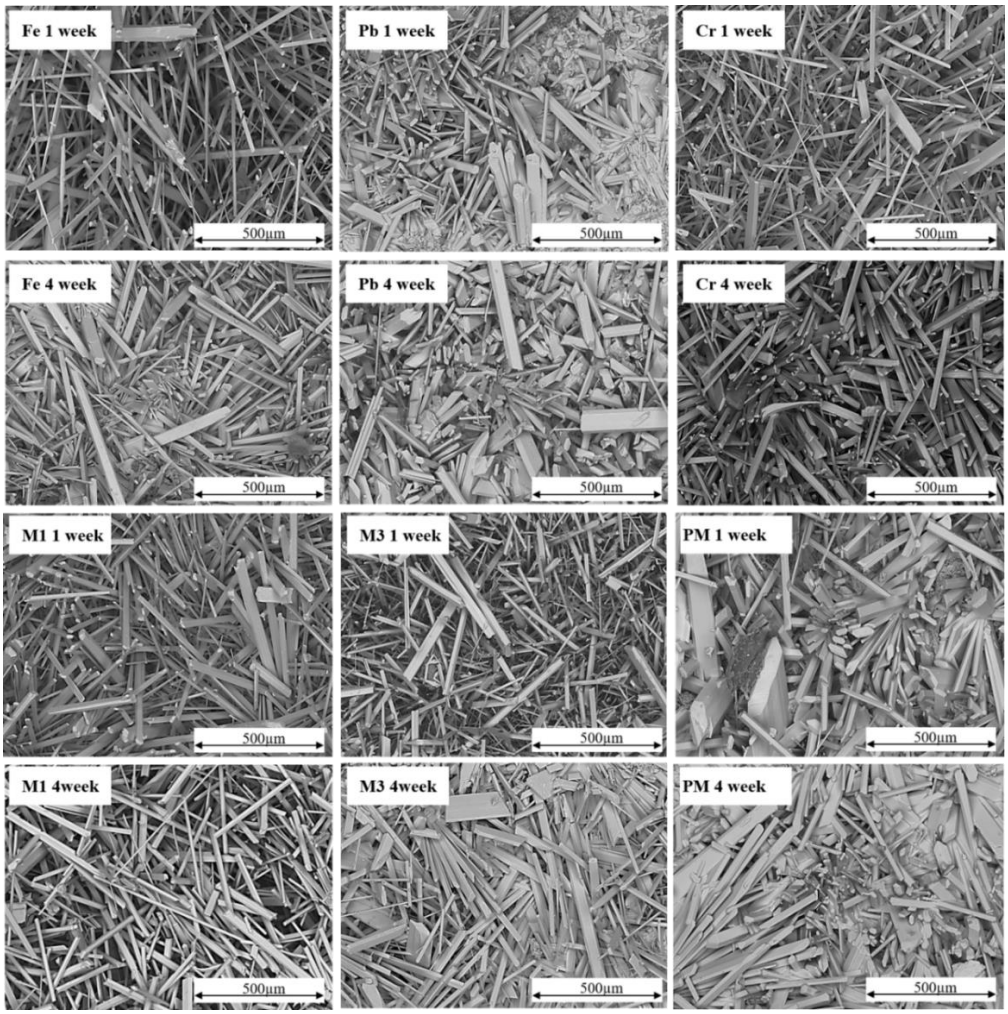

Fig 4. BSE images showing the different observations made on the surface of representative samples (Fe, Pb; Cr, M1, M2 and PM2.5) taken after the first and fourth week of exposure (scale bars 100 µm).

As observed with the stereomicroscope, PM2.5 (Fig. A2 supplementary materials) samples display the presence of larger crystals compared to other specimens, already in the first week. In some areas of specific samples (Fig. 4, e.g. PM2.5 and M3 and Pb), the crystals show up as aggregates with a tubular or lamellar hexagonal base habit. Instead, other specimens taken in the first week of exposure show small, thin acicular and needle-like gypsum crystals intertwined on the surface with a fibrous distribution (Fig. 4, e.g. Cr, M1; M3).

Mock-up samples taken after the fourth week of exposure behave differently: while some show large crystal growth and better interlocking radial distribution (Fig. 4, e.g. Pb, M3 and PM 2.5), others do not seem to undergo significant changes, except in crystal thickness (Fig. 4, e.g. Fe, Cr, M1 samples).

This evidence suggests a different role of the various metals in the sulphation process; however, having worked with high concentrations of SO_2 inside the accelerated ageing chambers, it is difficult to highlight clear differences among the samples. In fact, the formation of new gypsum crystals over the whole sampling period was observed in areas which tended to overlap with previously formed crystals (Fig. A3 supplementary materials). Furthermore, SEM does not provide information on the possible growth of gypsum crystals in the bulk of the specimens. In this regard, a more extensive study is currently underway, which will clarify any observations made on the cross-sections of the mock-ups.

Finally, EDX maps were also performed for each sample to verify the elemental composition. The analysis of the different maps confirmed that the surface is mainly composed of sulphur and calcium (Fig. 5).

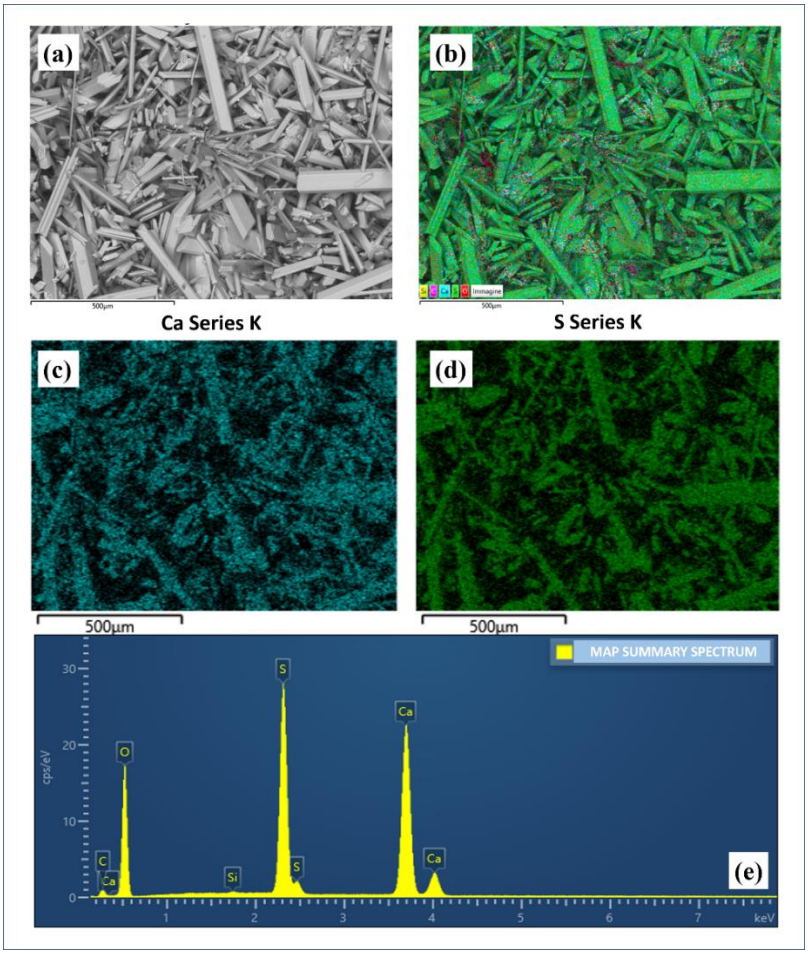

Fig 5. Representative SEM-EDX images of the sample treated with Pb taken at 4 weeks of exposure. (a) BSE image showing the analysed air gypsum crystals of the sample; (b) SEM-EDX false-color map obtained from the analysed surface of the sample (scale bars 500 µm); (c) SEM-EDX false-color map of Ca (scale bars 500 µm); (d) False-colour SEM-EDX map of S (scale bars 500 µm); e) EDX spectrum obtained from the analysed surface of the sample.

3.3.Colorimetric analysis

Colorimetric analyses were performed on the samples following the deposition of solutions/PM 2.5, prior to their introduction in the climatic chamber, and after every week of exposure. The colour difference was quantified and used as a parameter indicating gypsum formation. Specifically, it was hypothesized that an increase in the L*(increase in brightness) coordinate over time could be correlated with an increase in gypsum on the surface. This is because the addition of graphitic carbon prior to exposure in the climatic chambers causes a decrease in surface brightness with respect to the original substrate, which can now be differentiated from gypsum.

Hence, a normalized index ($vL(i,h)$) was introduced to compare the colour change induced by the different deposited solutions. This is expressed as the percentage variation of the increase of brightness L of the mixture h at week i,:

$$vL(i,h)\% = \frac{L(i)-L(post)}{L(post)} * 100.$$

where,

$L(i)$ = Average L value calculated on the specimen surface after exposure in the accelerated ageing test during the different weeks of exposure;

$L(post)$ = Average L value calculated on the surface of the test specimen after treatment with graphitic carbon and solutions.

Figure 6 shows the percentage values of vL.

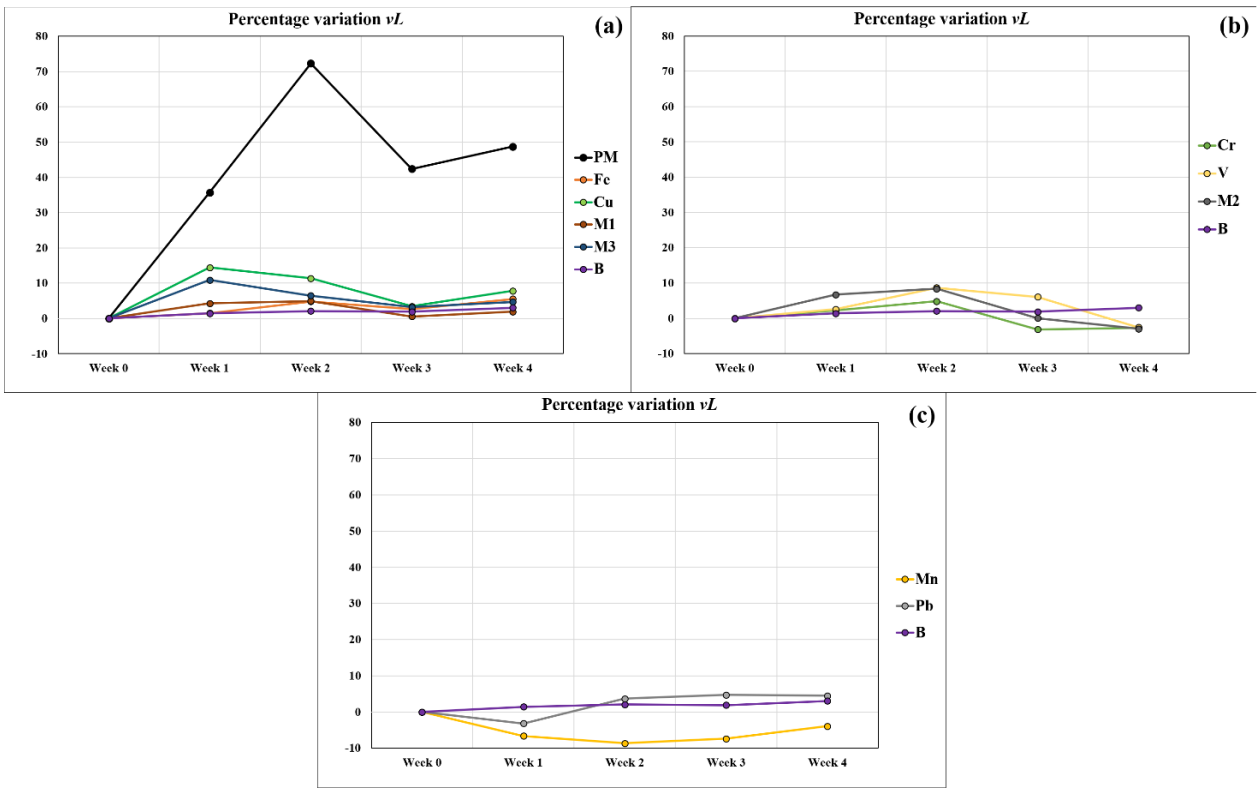

Fig. 6 Graphs reporting the change in brightness (vL%) obtained during the 4-week exposure in the accelerated ageing a) samples PM, Fe, Cu, M1, M3, B; b) samples Cr, V, M2, B; c samples Mn, Pb, B.

As expected, vL % values for blank (B) samples remain constant throughout the different exposure weeks indicating that there is no significant colour difference between the carbonate substrate and the newly formed gypsum. Fig 6a shows that the PM2.5-treated specimens are associated with a greater variation of this index and greater absolute values. This is especially the case in the first and second week of exposure, where a large increase was observed. Differently, a decrease in vL % was registered after the third week and a small increase after the fourth one. The high vL % can be attributed to a high amount of gypsum crystals being formed, due to a high catalytic action caused by the more complex chemical composition of PM 2.5 which resulted also in a high increase of the L* parameter in the first weeks.

A similar trend was observed for Fe, Cu, M3, and M1 (Fig. 6a), despite the overall values being lower than PM 2.5. A vL % increase was registered in the first week of exposure, which continued over the second one, then decreased in the third week and again increased slightly, in the fourth week. The increase during the last week can be explained by the advancement of the degradation and sulphation process, i.e. the tendency to continuously form new gypsum (white in colour) in the surface layer, as observed by SEM (Fig. A3 supplementary materials).

For the specimens treated with M2, V and Cr (Fig. 6b), there is a progressive increase over the first two weeks followed by a decrease in the vL % value during the third and fourth weeks (negative

values obtained in week 3 and week 4 for M2 and Cr and only in week 4 for V). The decrease in brightness observed over the third and fourth week can be attributed to the sulphation process that occurred on these surfaces. As observed via SEM, the gypsum crystals formed in the early weeks are small, thin, and not aggregated (Fig. 3). In the subsequent weeks, sulphation leads to thickening of the crystals, which become more compact as they grow and can encapsulate graphitic carbon, bringing it to the surface. Indeed, as reported in some studies conducted on samples of real black crusts (Barca et al., 2014; Belfiore et al., 2013; Del Monte and Sabbioni, 1984; La Russa et al., 2013), carbon particles may be present on the surface, not only due to possible recent deposition, but also due to the thickening of gypsum crystals, which may transport carbonaceous particles from the inner to the outer layers.

For the Pb-treated specimens (Fig. 6c), a negative vL % value was observed after the first week indicating no catalytic activity in the sulphation process. This behaviour was reversed over the following weeks where a vL % increase was observed. This steady increase may be ascribed to a delayed catalytic action, which increases steadily over time, as previously observed through macroscopic observations.

A unique behaviour was observed for the sample treated with Mn (Fig. 6c). In fact, results show consistently negative *vL* % variation values over the weeks with a slight increase only during the third and fourth weeks, suggesting the lowest catalytic action for this metal under these experimental conditions.

3.4. Ion chromatography analysis

Analyses by Ion Chromatography (IC) made it possible to assess the concentration of sulphate ions (which identify the presence of gypsum salt) present on the surface of the specimens during the four weeks of exposure. IC registered the presence of sulphate ions in all the samples over the four weeks , confirming the presence of gypsum formed in the accelerated ageing tests (Fig. 7).

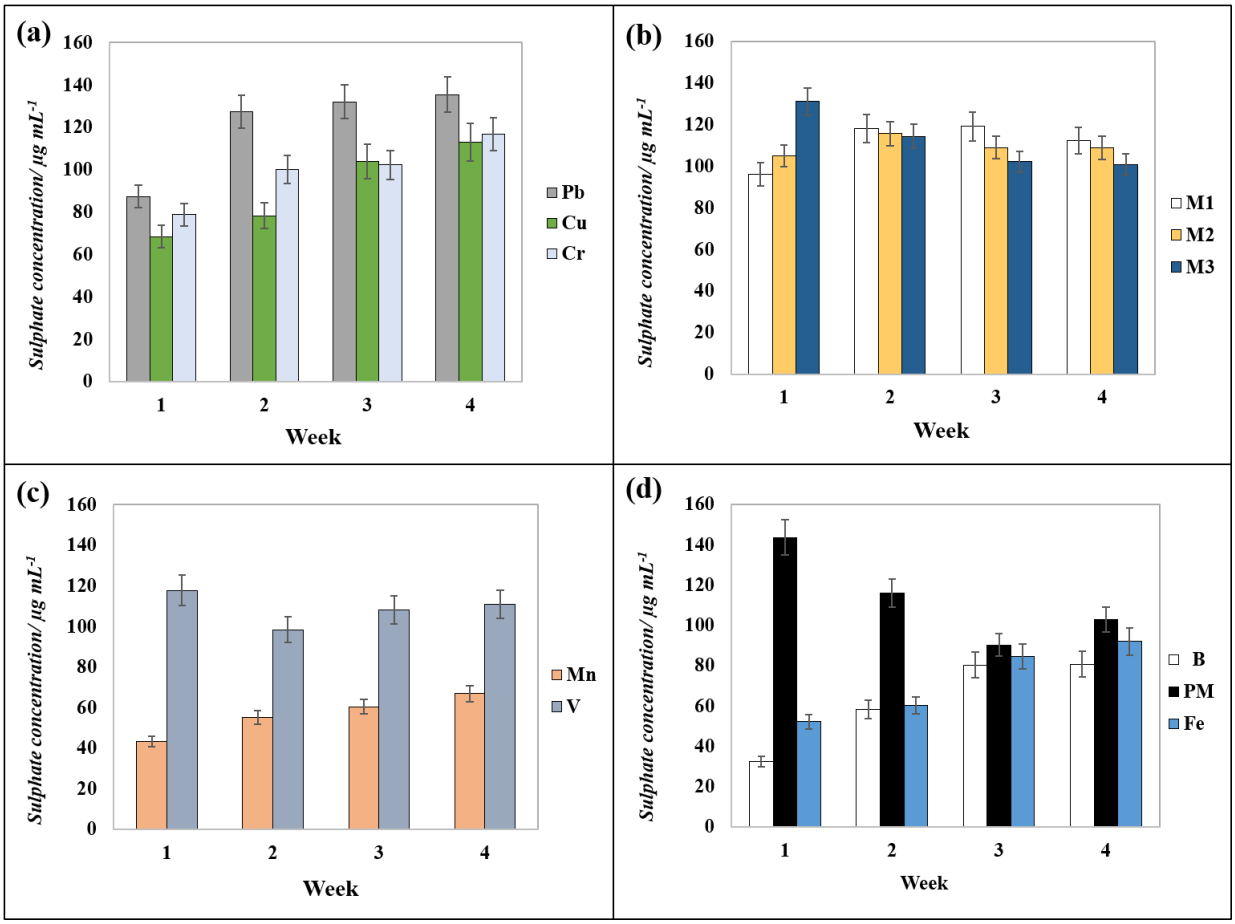

Fig. 7 Histograms of sulphate concentrations on different types of samples during the four weeks of exposure. (a) series with Pb, Cu, Cr; (b) series with M1, M2, M3; (c) series with Mn, V; (d) series with B, PM, Fe.

The highest values were obtained in the first week for specimens treated with PM 2.5 and M3 (143.65 and 131.01 µg/mL, respectively). This indicates that, under these experimental conditions, the combination of several metals promotes a higher catalytic action than taken individually. The lowest concentrations were observed for the reference sample B (untreated blank; 32.59 µg/mL; Fig. 7a) and for the mock-up samples treated with Fe and Mn (43.36 and 52.13 µg/mL, respectively; (Fig. 7d,c). Results for sample B confirm that the presence of a metal catalyst is essential in increasing the sulphation rate. Moreover, albeit limited, that the presence of gypsum also in the blank samples shows that the harsh conditions inside the chambers allow its formation also in the absence of a catalyst. With regards to Fe and Mn, results indicate that these metals do not play a key role in the sulphation process under these experimental conditions in the first week.

In the second week, the values of PM 2.5 and M3 decrease (114.33 and 115.96 µg/mL, respectively; Fig. 7b,d), probably because the accelerated degradation observed in the first week led to more extensive degradation, favouring the formation of gypsum also within the marble bulk. The same observation can be extended to the M1 and M2 mixtures (Fig. 7b) in which the SO_4^{2-} concentration increased from the first week (96.01 and 104.83 µg/mL, respectively) to the second week (118.09 and 115.62 µg/mL, respectively) followed by a decrease during the third week (119.04 and 108.95 µg/mL, respectively) and, although slightly, over the fourth week (112.14 and 108.76 µg/mL, respectively).

In contrast, the concentration of sulphate ions increased from the first to the fourth week in the samples treated with Pb (127.35 µg/mL;) as well as in the specimens treated with Cu and Cr (78.22 and 100.16 µg/mL, respectively) (Fig.7a). This result suggests that these metal cations have a delayed, but continuous catalytic action. The fact that no decrease in sulphate ion concentrations was observed indicates that sulphation develops less aggressively than in other mock-up samples, such as PM 2.5 and M3, where degradation is favoured at the expense of bulk. In fact, the maximum sulphate concentration reached in week 4 for the sample treated with Pb is comparable to the one reached in week 1 for the PM.2.5 sample. Extending the time frame of the experiment would probably lead to a similar decrease in sulphate ion concentrations also for the Pb sample, which would be ascribable to the penetration of gypsum into the marble sample.

Samples treated with Fe present small increases in sulphate ion concentrations over the last three weeks, lower than the other mock-ups (Fig. 7d). This confirms that this metal alone does not play a major role in the sulphation process. Indeed, as shown by Boke et al., 1999, it is likely that Fe has no influence on the catalytic oxidation of calcium sulphite hemihydrate into gypsum. Although ferric ions are known as active catalysts on the oxidation of SO_2 in the aqueous phase (Grgicet al. 1992), they probably do not have a high effect in the formation of gypsum under these operating conditions.

Finally, the samples treated with Mn (Fig. 7c) showed the lowest concentrations of sulphate ions over the last three weeks even compared to the untreated B sample. In fact, after the fourth week, the concentration obtained for the Mn sample was 66.93 µg/mL while that obtained from the analysis of the B sample was 80.68 µg/mL. This finding confirms that Mn seems to act as an inhibitor of sulphation process.

A different index, the *growth rate* ($G(i,h)$), was developed to evaluate the variation rate of sulphate ions. This index measures the concentration normalized by the number of days of exposure and is defined as:

$$G(i,h) = \frac{C_{si}(7*i)}{7*i},$$

where $G(i,h)$ is the growth rate of the sulphate ions in the solution h at week i, and $C_{si}(7*i)$ is the sulphate ion concentration at the $7*i$ day.

Results are shown in Figure 8a-b.

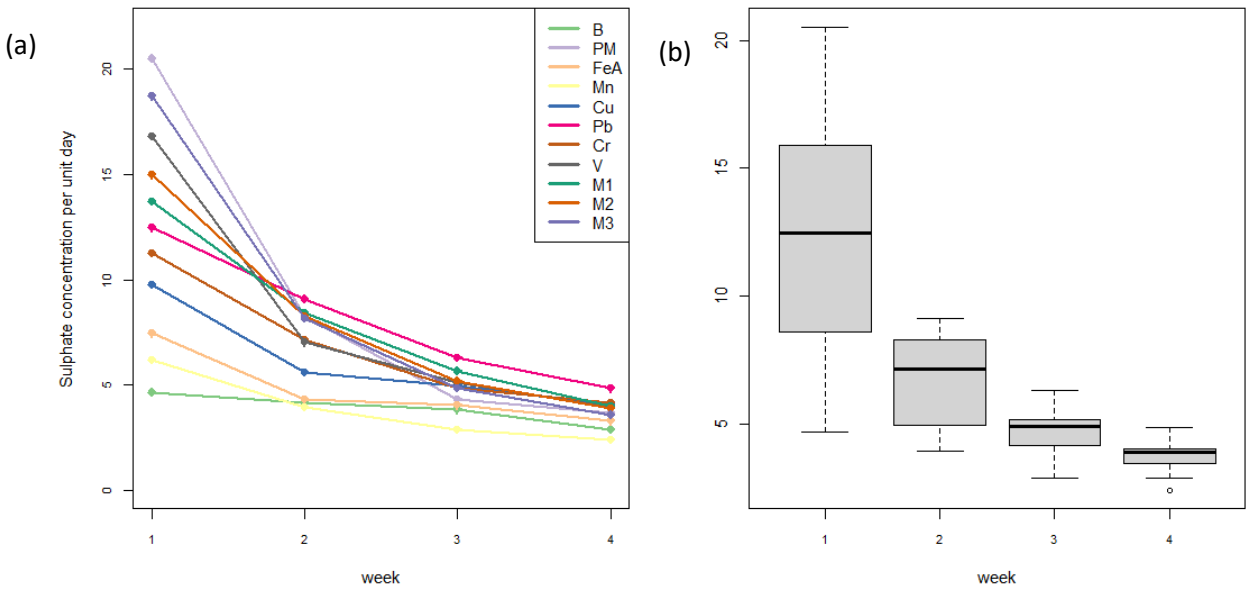

Fig 8: Sulphate concentration *growth rate*. (a) Comparison for each metal or mixture. (b) Boxplot of the distribution of the growth rates at week 1,2,3,4.

Figure 8a is a direct comparison of the sulphate concentration growth rate for the different specimens at the different weeks of observation. The highest reaction speed occurs during the first week, while a saturation effect is evident at the 4th week. It is important to note that this observation solely considers surface-level phenomena and does not account for potential gypsum penetration into the substrate.

The blank sample (B) shows a constant growth rate from the first to the fourth week. The specimen treated with Mn is the only one showing lower growth rates in the second, third and fourth weeks of exposure. This suggests that this metal acts initially as a catalyst and then as an inhibitor. The growth rate of Fe samples follows a similar trend and is comparable to the growth rate of the blank except for the first week, indicating once again a limited catalytic action for this metal.

A different trend can be observed for solutions treated with PM, M3 and V, which produce the fastest growth during the first week and a constant decrease in the following weeks

Instead, samples treated with Cu and Cr show a positive catalytic action during the entire sampling period, but the growth rate remains constant after the second week as was the case for Fe and Mn.

With regards to M1 and M2 mixtures, the behaviour observed confirms the results of previous analyses. Both have a positive catalytic action during the entire period and, if compared to the more reactive M3 mixture, it is possible to notice a slower reaction during the first week, a similar growth rate at week 2, and a greater rate rate for the final two weeks. This confirms the greater reactivity of M3, which reaches saturation quicker, and a more constant catalytic action for the other two mixtures.

Finally, the catalytic action of Pb is delayed at week 1, but in the following weeks the growth is constant and reaches almost the same level as PM at week 1.

In Figure 8b the boxplots of the growth rates of the sulphate concentration for each week of exposure are shown. There is a large initial variability in week 1, in which the differences between the metal cations are magnified. The growth rates tend to eventually homogenize with increasing exposure time.

The mathematical models currently present in literature describing the sulphation of calcium carbonate (i.e. Aregba-Driollet at al. 2004, Arceci at al, 2023) predict rapid gypsum crust formation in the case of accelerated reaction with a time-dependant limit of the reaction rate This is in agreement with the performed experiments in which gypsum crust formation occurs quickly and reaction velocity slows down approaching saturation.

3.5.XRPD analysis

XRPD analysis was performed to assess the crystalline phases. Specifically, investigations were conducted on the powders of untreated and exposed samples, on the powder removed from the surface of the mock-up samples taken during the four-week exposure, and on the surface of the specimens after plaster removal to check for possible penetration into the marble bulk.

The results indicate that all the powder samples already showed the characteristic mineralogical phases of calcium sulphate dihydrate with its characteristic peaks (most intense peak at low angle around 10°), but also calcium carbonate with less intense peaks (Fig. A4 supplementary materials and Fig. 9a). The presence of the latter, on the other hand, suggests that in the powder taken from the surface, a part of the substrate may also have been removed unintentionally because of its degradation, which often leads to intracrystalline decohesion of calcite crystals (Barca et al., 2015; Bonazza et al., 2005).

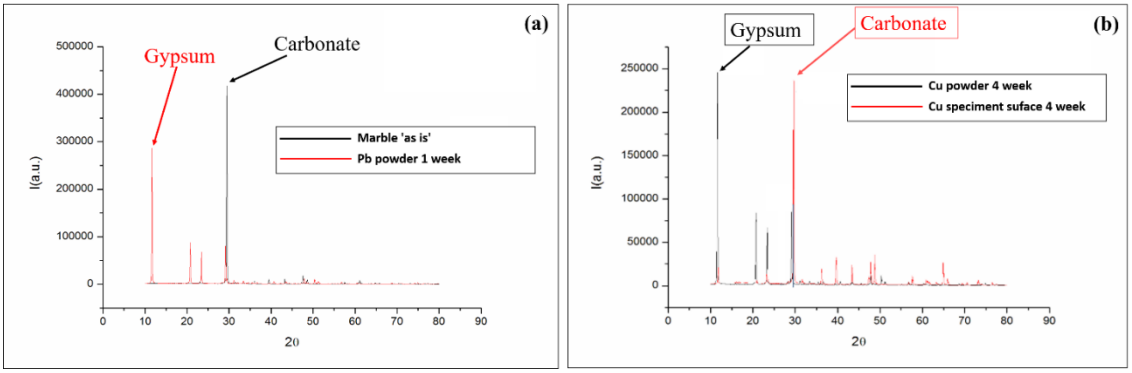

Fig. 9 (a) XRPD comparison between the patterns of marble *as is* and that of the dust taken after the first week of exposure; (b) Comparison between the patterns of the powder removed from the surfaceand the surface after powder removal after 4 weeks exposure.

The diffractogram of blank samples (Fig. 9a) indicates the presence of only calcium carbonate (most intense peak present at about 30°), in contrast to all samples treated with metal solutions or PM where the crystalline phases of gypsum predominate as early as the first week. To better understand the relationship between the formation of gypsum and the degradation of the carbonate stone substrate, the underlying surface of the specimens was also analysed by conducting investigations after removal of the powder (Fig. 9b). The results show a reversal in the intensities of the gypsum and calcite peaks: the latter being more intense than the former (Fig. 9b). Although less intense, the presence of gypsum in the underlying layerssuggests that the degradation process extends beyond the surface, affecting the marble bulk. Such deterioration likely leads to the infiltration of gypsum into the substrate, resulting in intracrystalline decohesion of the calcite crystals, as discussed earlier. SEM-EDX observations (Fig. 5A in the Supplementary Material) conducted on the sample surfaces post-gypsum patina removal reveal significant degradation, intensifying over the 4-week exposure period. In Fig. 5Aa,b, the surface of a representative specimen is observed at different magnifications (60X and 150X), highlighting small cracks containing crystallization nuclei of gypsum above the calcite substrate. To confirm these observations, false-colour SEM-EDX maps were generated, showing a clear overlap in the areas containing sulphur and calcium. Additionally, EDX acquisitions following a linear trajectory (500µm) along the sample surface (Fig. 6A in the Supplementary Material) uncovered sulphur presence within small cracks.

3.6. Comparison of Obtained Data

The present study evaluated the different catalytic ability of heavy metals commonly found in particulate matter towards the sulphation of marble surfaces. Solutions of individual metals, metal mixtures and PM2.5 were tested on marble specimens under accelerated aging conditions. By integrating results from macroscopic observations, SEM-EDX analysis, colorimetric measurements, ion chromatography, and XRPD, a comprehensive understanding of the sulphation process and the catalytic action of the different heavy metals was achieved.

The results indicate that samples treated with the M3 (Fe^{3+}, Cu^{2+}, Mn^{2+}, Pb^{2+}, Cr^{3+}, V^{5+}) solution and PM2.5 were associated with a significantly higher gypsum formation, with abundant and large crystals as early as the first week of exposure. Conversely, samples treated with solutions of Pb, Cu, and Cr show only a moderate gypsum formation, characterized by a slower but constant catalytic action over time. This suggests that all the aforementioned metals are able to catalyse effectively the sulphation reaction, but the synergistic effect is greater than each of them acting individually. In contrast, Fe and Mn-treated samples showed minimal catalytic activity.

Colorimetric analysis confirms that M3 and PM2.5 treated samples have higher vL% values, reflecting greater gypsum formation. In contrast, Fe and Mn-treated samples consistently show lower vL% values, indicating reduced gypsum formation. Ion chromatography further supported these

findings, showing higher sulphate ion concentrations in PM2.5 and M3-treated samples, while Fe and Mn-treated samples have lower sulphate concentrations, highlighting the limited role of these metals in promoting gypsum formation. XRPD analysis reveals that gypsum forms primarily on the surface, but also within the marble substrate, suggesting that degradation is able to extend also in the bulk of the marble. However, further testing is needed to validate this observation.

In summary, the data suggests that the M3 mixture (containing all selected metals) and PM2.5 are the most effective catalysts for gypsum formation due to the synergistic effect of the metals. Pb, Cu, and Cr show a delayed but constant catalytic action, while Fe and Mn show minimal catalytic activity under the tested experimental conditions.

Conclusions

The aim of this study was to understand the role of specific heavy metals in black crust formation mechanisms on monumental stone. Carrara marble mock-ups underwent accelerated aging in two climate chambers (SO_2-corrosion chamber and solar irradiation chamber) to simulate outdoor conditions. The tested specimens were treated with solutions of individual metal cations, mixtures and PM2.5 extracted from ambient air filters. Samples were analysed before and after every week of accelerated aging exposure in the chambers using SEM-EDX, colorimetry, IC, and XRPD. Colorimetric quantitative measurements were obtained as the percentage variation of the brightness (L) increase for every mixture and week of exposure. Also, the growth rate of the sulphate ion concentration was calculated for every solution and week of exposure for quantitative analyses. The results showed that the specimens treated with mixtures of multiple metal cations and PM 2.5 samples, had higher sulphation rates. Some metals (e.g., Pb, Cu, Cr) became more active over time, while Mn was the least reactive. Sulphate concentration peaked after the first week, then reached a saturation point by the fourth week, indicating deeper substrate penetration. Additional tests with modified experimental conditions are in progress aiming to better clarifying the catalytic role of individual metals.

Funding:

This work was supported by the Project SOE-SCICULT (Modellizzazione matematica e analisi SCIentifica per i beni CULTurali: previsione e prevenzione del degrado chimico e meccanico di pietre monumentali in ambienti outdoor) [Bando Seal of Excellence, n.1093, 2020] funded by Università degli Studi di Milano.

References

Allen, G.C., El-Turki, A., Hallam, K.R., McLaughlin, D., Stacey, M., 2000. Role of NO_2 and SO_2 in degradation of limestone. Br. Corros. J. 35,1, 35-38. Doi:10.1179/000705900101501047.

Amoroso, G.G., Fassina, V., 1983. Stone decay and conservation: atmospheric pollution, cleaning, consolidation and protection. Elsevier, Amsterdam.

Arceci, F., Giordano, L.M., Maurelli, M., Morale, D., Ugolini, S., 2023. A Randomness in a nonlinear model of sulphation phenomenaIn: Mathematical Modeling in Cultural Heritage, MACH2021, (G. Bret, C. Cavaterra, M. Solci, M. Spagnuolo Eds). Springer INdAM Series, 55, 31–50. https://doi.org/10.1007/978-981-99-3679-3_3.

559 Aregbda-Driollet, D., Diele, F., Natalini, R., 2004. A mathematical model for the sulphur dioxide
560 aggression to calcium carbonate stones: numerical approximation and asymptotic analysis. SIAM J.
561 Appl. Math. 64 (5), 1636-1667. https://www.jstor.org/stable/4096089.
562 Ausset, P., Del Monte, M., Lefevre, R.A., 1999. Embryonic sulphated black crusts on carbonate rocks
563 in atmospheric simulation chamber and in the fild: role of carbonaceous fly-ash. Atmos. Environ. 33,
564 1525-1534. doi:10.1016/S1352-2310(98)00399-9.

565 Ausset, P., Crovisier, J.L., Del Monte, L., Furlan, V., Girardet, F., Hammecker, C., Jeannette, D.,
566 Lefevre, R.A. (1996) Experimental study of limestone and sandstone sulphation in polluted realistic
567 conditions: the Lausanne Atmospheric Simulation Chamber (LASC). Atmos. Environ. 30,18, 3197-
568 3207. https://doi.org/10.1016/1352-2310(95)00495-5.

569 Barca, D., Comite, V., Belfiore, C.M., Bonazza, A., La Russa, M.F., Ruffolo, S.A., Crisci, G.M.,
570 Pezzino, A., Sabbioni, C., 2014. Impact of air pollution in deterioration of carbonate building
571 materials in Italian urban environments. Appl. Geochem. 48, 122–131.
572 https://doi.org/10.1016/j.apgeochem.2014.07.002.

573 Barca, D., Comite C., Belfiore, C.M., Bonazza, A., La Russa, M.F., Ruffolo, S.A., Crisci, G.M.,
574 Pezzino, A., Sabbioni, C., 2014; Impact of air pollution in deterioration of carbonate building
575 materials in Italian urban environments. Applied Geochemistry 48, 122–131.
576 http://dx.doi.org/10.1016/j.apgeochem.2014.07.002.

577 Belfiore, C.M., Barca, D., Bonazza, A., Comite, V., La Russa, M.F., Pezzino, A., Ruffolo, S.A.,
578 Sabbioni, C., 2013. Application of spectrometric analysis to the identification of pollution sources
579 causing cultural heritage damage. Environ. Sci. Pollut. Res. 20, 8848–8859. doi: 10.1007/s11356-
580 013-1810-y.

581 Beilke, S., Gravenhorst, G., 1978. Heterogeneous SO_2—oxidation in the droplet phase. Atmos.
582 Environ. 12, 231 – 239. https://doi.org/10.1016/0004-6981(78)90203-2.

583 Bonazza, A., Sabbioni, C., Ghedini, N., Gobbi, G., 2007. Blackening as major atmospheric pollution
584 effect on monuments. Pollution Atmosphérique-Numèro Spècial, 7-12.

585 Bonazza A., Sabbioni, C., Ghedini, N., 2005. Quantitative data on carbon fractions in interpretation
586 of black crusts and soiling on European built heritage. Atmos. Environ. 39, 2607–2618. doi:
587 10.1016/j.atmosenv.2005.01.040.

588 Boke, H., Gokturk, E.H., Caner-Saltik, E.N., Demirci, S., 1999. Effect of airborne particle on SO_2 –
589 calcite reaction. Appl. Surf. Sci. 140, 70-82. https://doi.org/10.1016/S0169-4332(98)00468-1.

590 Brandt, C., van Eldik, R., 1995. Transition metal-catalyzed oxidation of sulfur(IV) oxides:
591 atmospheric-relevant processes and mechanisms. Chem. Rev. 95, 19 – 190.
592 https://doi.org/10.1021/cr00033a006.

593 Beilke, S., Gravenhorst, G., 1978. Heterogeneous SO_2—oxidation in the droplet phase. Atmos.
594 Environ. 12, 231- 239. https://doi.org/10.1016/0004-6981(78)90203-2.

595 Bergomi, A., Comite, V., Della Pina, C., Cavaterra, C., Gianelle, V.L., Fermo, P., 2022. Development
596 of a new procedure for the assessment of particulate matter (PM) carbonaceous fraction on stone
597 materials exposed to atmospheric pollution. J Phys: Conf Ser, 2204(1), 012106.
598 https://doi.org/10.1088/1742- 6596/2204/1/012106.Brimblecombe, P., 1999. History of urban air
599 pollution. In: Finger J, Herter O, Palmer F (eds) Urban air pollution—European aspects. Kluver,
600 Dordrecht, 7–20.

601 Bugini, R., Laurenzi Tabasso, M., Realini, M., 2000. Rate of formation of black crusts on marble. A
602 case study. J. Cult. Herit. 1(2), 111-116. doi: 10.1016/S1296-2074(00)00161-8

Brimblecombe, P., 2000. Air pollution and architecture, past, present and future. J. Archit. Conserv. 6, 30–46. doi:10.1080/13556207.2000.10785268.

Cheng, J.R., Hwu, J.R., Kim, J.T., Leu, S.M., 1987. Deterioration of marble structures. The role of acid rain. Anal. Chem. 59, 104-106. https://doi.org/10.1021/ac00129a002

Cobourn, W.G., 1993. Laboratory measurements of sulfur dioxide deposition velocity on marble and dolomite stone surface. Atmos. Environ., vol. 27B, No. 2,193 – 201. https://doi.org/10.1016/0957-1272(93)90005-Q.

Comite, V., Miani, A., Ricca, M., La Russa, M.F., Pulimeno, M., Fermo, P. 2021. Int. J. Biomed. Res. The impact of atmospheric pollution on outdoor cultural heritage: an analytic methodology for the characterization of the carbonaceous fraction in black crusts present on stone surfaces. 201, p.111565. https://doi.org/10.1016/j.envres.2021.111565.

Comite, V., Alvarez de Buergo, M., Barca, D., Belfiore, C.M., Bonazza, A., La Russa, M.F., Pezzino, A., Randazzo, L., Ruffolo, S.A., 2017. Damage monitoring on carbonate stones: field exposure tests contributing to pollution impact evaluation in two Italian sites. Constr. Build. Mater. 152, 907-922. https://doi.org/10.1016/j.conbuildmat.2017.07.048.

Comite, V., Bergomi, B., Della Pina, C., Castellano, C., Borelli, M., Lombardi, C.A., Formenti, M., La Russa, M.F., Cavaterra, C., Fermo, P., 2022. Climatic chamber tests to evaluate the catalytic action of heavy metals in the sulphation process. 2022 IMEKO TC-4 International Conference on Metrology for Archaeology and Cultural Heritage, MetroArchaeo 2022, 294-299. doi: 10.21014/tc4-ARC-2022.05.

Delegou, E.T., Ntoutsi, I., Kiranoudis, C.T., Sayas, J., Moropoulou, A., 2018. Advanced and Novel Methodology for Scientific Support on Decision-Making for Stone Cleaning. In: Hosseini, M., Karapanagiotis, I. (eds) Advanced Materials for the Conservation of Stone. Springer, Cham. https://doi.org/10.1007/978-3-319-72260-3_14

Del Monte, M., Sabbioni, C., Vittori, O., 1981. Airborne carbon particles and marble deterioration. Atmos. Environ. 15, 645–652. doi:10.1016/0004-6981(81)90269-9.

Del Monte, M, and Sabbioni, C., 1984. Gypsum crust and fly ash particles on carbonatic outcrops. Arch. Met. Geoph. Biocl. Ser. B35, 105-111

Elfving, P., Panas, I., Lindqvist, O., 1994. Model study of the first steps in the deterioration of calcareous stone I. Initial surface sulphite formation on calcite. Appl. Surf. Sci.74, 1, 91-98. https://doi.org/10.1016/0169-4332(94)90103-1.

Fassina, V., 1988 Influenza dell'inquinamento atmosferico sui processi di degrado dei materiali lapidei. Bollettino d'Arte "Materiali lapidei-problemi relativi allo studio del degrado e conservazione Vol. I, Suppl. 41, 37-52.

Fermo, P., Goidanich, S., Comite, V., Toniolo, L., Gulotta D., 2018. Study and Characterization of Environmental Deposition on Marble and Surrogate Substrates at a Monumental Heritage Site. Geosci. 8(9), 349; https://doi.org/10.3390/geosciences8090349.

Fermo, P., Turrion, R.G., Rosa, M., Omegna, A., 2015. A new approach to assess the chemical composition of powder deposits damaging the stone surfaces of historical monuments. Environ. Sci. Pollut. Res. 22, 6262–6270. doi:10.1007/s11356-014-3855-y

Gavino, M., Hermosin, B., Verges-Belmin, V., Nowik, W., Saiz-Jimenez, C., 2004. Composition of the black crusts from the Saint Denis Basilica, France, as revealed by gas chromatography-mass spectrometry. J. Sep. Sci. 27,513-523. doi: 10.1002/jssc.200301626.

Giavarini, C., Santarelli, M.L., Natalini, R., Freddi, F., 2008. A non-linear model of sulphation of porous stones: numerical simulations and preliminary laboratory assessments. J. Cult. Herit. 9, 14-22. https://doi.org/10.1016/j.culher.2007.12.001.

Grgic, I., Hudnik, V., Bizjak, M., Levec, J. 1992 Aqueous S(IV) oxidation-II. Synergistic effects of some metal ions. Atmos. Environ. 26, 4, 571-577. https://doi.org/10.1016/0960-1686(92)90170-P.

Hutchinson, A.J., Johnson, J.B., Thompson, G.E., Wood, G.C., Sage, P.W., Cooke, M.J., 1992. The role of fly-ash particulate material and oxide catalysts in stone degradation. Atmos Environ Part A General Topics. 26, 15, 2795-2803. https://doi.org/10.1016/0960-1686(92)90017-F.

Lancia, A.B., Musmarra, D., Pepe, F., Volpicelli, G., 1991. Concentration profiles in the diffusional film in the calcium carbonate dissolution process. Chem. Eng. Sci. 46, 2507 - 2512. https://doi.org/10.1016/0009-2509(91)80044-Y

La Russa, M.F., Belfiore, C.M., Comite, V., Barca, D., Bonazza A, Ruffolo, Crisci, G.M., Pezzino, A., 2013. Geochemical study of black crusts as a diagnostic tool in cultural heritage. Appl. Phys. A: Mater. 113, 1151–62. doi:10.1007/s00339-013-7912-z.

Maravelaki-Kalaitzaki P., 2004. Black crusts and patinas on Pentelic marble from the Parthenon and Erechtheum (Acropolis, Athens): characterization and origin. Analytica. Chimica. Acta. 532, 187-198. doi:10.1016/j.aca.2004.10.065.

Martins, C.R., Neto, C.A.C., Alves, J.F., de Andrade, J.B., 1999. Oxidation of sulfur (IV) by oxygen in aqueous solution: role of some metal ions. J. Braz. Chem. Soc. 10, 6, 45 - 55. https://doi.org/10.1590/S0103-50531999000600006

McAlister, J.J., Smith, B.J., Neto, J.B., Simpson, J.K., 2005. Geochemical distribution and bioavailability of heavy metals and oxalate in street sediments from Rio de Janeiro, Brazil: a preliminary investigation. Environ. Geochem. Health. 27,429–41. doi: 10.1007/s10653-005-2672-0.

McAlister, J.J., Smitha, B.J., Tőrők, A., 2006. Element partitioning and potential mobility within surface dusts on buildings in a polluted urban environment, Budapest. Atmos. Environ. 40, 6780–90. https://doi.org/10.1016/j.atmosenv.2006.05.071

McAlister, J.J., Smitha, B.J., Tőrők, A., 2008, Transition metals and water-soluble ions in deposits on a building and their potential catalysis of stone decay. Atmos. Environ. 42, 7657–68. https://doi.org/10.1016/j.atmosenv.2008.05.067.

Novakov, T., Chang, S.G., Harker, A.B., 1974. Sulfates as pollution particulates: catalytic formation on carbon (soot) particles. Science 186, n 4160, 259 - 261. doi: 10.1126/science.186.4160.259.

Price, C. A., & Brimblecombe, P., 1994. Preventive conservation in museums. Part II. Development of an environmental control system. Studies in Conservation, 39(4), 204-209. DOI: 10.1179/sic.1994.39.4.204

Rodriguez-Navarro C., Sebastian, E. 1996. Role of particulate matter from vehicle exhaust on porous building stones (limestone) sulphation. Sci. Total Environ. 187,2, 79-91. https://doi.org/10.1016/0048-9697(96)05124-8.

Ruffolo, S.A., Comite, V., La Russa, M.F., Belfiore, C.M., Barca, D., Bonazza, A., Crisci, G.M., Pezzino, A., Sabbioni, C., 2015. An analysis of the black crusts from the Siville Cathedral: a challenge to deepen the understanding of the relationships among microstructure, microchemical features and pollution sources. Sci. Total Environ. 502, 157-166. DOI: 10.1016/j.scitotenv.2014.09.02.

Sada, E., Kumazava, H., Hashizume, I., Nishimura, H., 1982. Absorption of dilute SO2 into aqueous slurries of CaSO3. Chem. Eng. Sci. 37, 1432 – 1435. https://doi.org/10.1016/0009-2509(82)85019-7

Sabbioni, C.C., Zappia, G., Ghedini N., Riontino C., 1997. Effects of air pollution on materials of artistic interest. International Conference on Air Pollution – Proceedings. 629-638. ISSN 1743-3541.

Spiker, E.C., Hosker, R.P., Comer, V.J., White Were, J.R., Jr R.W., Harmon, F.L., Gandy, G.D., Sherwood S.I., 1992. Environmental chamber for study of the deposition flux of gaseous pollutants to material surface. Atmos. Environ., 26A, 16, 2885 – 2892. https://doi.org/10.1016/0960-1686(92)90280-X.

Spiker, E.C., Hosker, R.P., Weintraub, V.C., Sherwood, S.I., 1995. Laboratory study of SO_2 dry deposition on limestone and marble: effects of humidity and surface variables. Way. Air Soil Poll., vol. 85, 2679-2685. doi: 10.1007/BF01186239

Toniolo, L., Zerbi, C.M., Bugini, R., 2009. Black layers on historical architecture. Environ. Sci. Pollut. Res. 16, 218-226. doi: 10.1007/s11356-008-0046-8.

Turkington, A.V., Smith, B.J., & Whalley, W.B., 1997. Short-term stone surface modification; an example from Venice. Proceedings of the 4th international symposium on the conservation of monuments in the Mediterranean basin. Technical chamber of Greece, Rhodes 1, 359–372.

Verges-Belmin V., 1994. Pseudomorphism of gypsum after calcite, a new textural feature accounting for the marble sulfation mechanism. Atm Environ., 28(2), 295-304. https://doi.org/10.1016/1352-2310(94)90104-X.

Vidal, F., Vicente, R., Mendes, Silva, J., 2019. Review of environmental and air pollution impacts on built heritage: 10 questions on corrosion and soiling effects for urban intervention. J. Cult. Herit. 37, 273-295. https://doi.org/10.1016/j.culher.2018.11.006.

Wittkowski, R., Schultze, D., & Rüdrich, J., 2014. Investigation of the weathering behavior of natural building stones under controlled environmental conditions. Environ. Earth Sci., 72(4), 1137-1150. DOI: 10.1007/s12665-014-3228-0.

Zappia, G., Sabbioni, C., Riontino, C., Gobbi, G., Favoni, O., 1998. Exposure tests of building materials in urban atmosphere. Sci. Total Enviro. 224, 235–244. doi:10.1016/S0048-9697(98)00359-3.